Research Square

Preprints are preliminary reports that have not undergone peer review.
They should not be considered conclusive, used to inform clinical practice,
or referenced by the media as validated information.

Integrated GWAS and Transcriptome Analysis Identifies Candidate Genes for Seedling-Stage Drought Tolerance in Indica Rice

Kaixuan He

623950736@qq.com

Hunan Agricultural University

Yongxin Li

Hunan Agricultural University

Zijie Liu

Hunan Agricultural University

Hexing Yin

Hunan Agricultural University

Hongyan Zhang

Hunan Agricultural University

Deze Xu

Hubei Academy of Agricultural Sciences

Xingfei Zheng

Hubei Academy of Agricultural Sciences

Lanzhi Li

Hunan Agricultural University

Research Article

Keywords: Rice seedling, Drought tolerance, Genome-wide association studies, Transcriptome analysis

Posted Date: March 31st, 2026

DOI: https://doi.org/10.21203/rs.3.rs-9077877/v1

License: This work is licensed under a Creative Commons Attribution 4.0 International License.
Read Full License

Additional Declarations: No competing interests reported.

Integrated GWAS and Transcriptome Analysis Identifies Candidate Genes for Seedling-Stage Drought Tolerance in *Indica* Rice

Kaixuan He[1,†], Yongxin Li[1,†], Zijie Liu[1], Hexing Yin[1,2], Hongyan Zhang[3,4], Deze Xu[5], Xingfei Zheng[5]*, Lanzhi Li[1]*

[1]Hunan Engineering & Technology Research Center for Agricultural Big Data Analysis & Decision-making, College of Plant Protection, Hunan Agricultural University, Changsha 410128, China

[2] Huazhi Biotechnology Co. Ltd, Changsha 410125, China

[3] College of Information and Intelligence, Hunan Agricultural University,Changsha, 410128, Hunan, China

[4] Department of Interdisciplinary Science and Smart Seed Industry Equipment, Yuelushan Laboratory, Changsha, 410128, Hunan, China

[5]Hubei Key Laboratory of Food Crop Germplasm and Genetic Improvement, Food Crop Institute, Hubei Academy of Agricultural Sciences, Wuhan 430064, China

[†]Kaixuan He and Yongxin Li have contributed equally to this work

*Correspondence

Xingfei Zheng:

zhengxingfei415@163.com

Lanzhi Li:

lancy0829@163.com

Abstract

Drought stress is a major constraint on rice productivity, especially at the seedling stage. In this study, we evaluated 283 *indica* rice accessions adapted to the middle and lower Yangtze River region for seedling-stage drought tolerance using four morphological traits: leaf senescence resistance index, leaf wilting score, plant height, and root length. A comprehensive drought tolerance metric (CDTM) was developed to integrate these traits, leading to the identification of ten superior drought-tolerant accessions. Genome-wide association study (GWAS) revealed 128 significantly associated SNPs, mapping to 133 candidate genes for drought-related traits. Transcriptome analysis of drought-tolerant and drought-sensitive cultivars under PEG-induced stress showed distinct expression profiles, with differential expression enriched in pathways related to fatty acid degradation, amino acid metabolism, and hormone signaling. By integrating GWAS and transcriptome analysis, we prioritized 12 core candidate genes repeatedly associated with multiple drought-related traits, six of which were further validated using an independent drought-stress transcriptome dataset from the water-saving and drought-resistant variety *Hanyou 73* under drought stress. Alternative splicing analysis revealed a significant skipped exon event in *Os03g0700700* under drought stress. Our findings provide valuable genetic resources and candidate genes for molecular breeding amied at enhancing seedling-stage drought tolerance in rice breeding programs.

Keywords：Rice seedling; Drought tolerance; Genome-wide association studies; Transcriptome analysis

Introduction

Ensuring stable rice production is fundamental to global food security. However, increasingly frequent and severe drought events pose a major threat to sustainable rice production. Compared with most upland crops, rice typically requires two to three times more irrigation water. Consequently, escalating climatic stress and water scarcity have intensified the demand for high-yielding and drought-tolerant rice varieties (Shi et al. 2020).

The seedling stage is particularly sensitive to drought stress in rice (Panda et al. 2021). Water deficit at this developmental phase impairs seedling establishment and suppresses root and shoot growth, and can further disrupt physiological performance, thereby adversely affecting subsequent tillering, flowering, and grain formation, ultimately reducing yield (Bhandari et al. 2022; Jarin et al. 2024). Therefore, seedling-stage drought tolerance not only reflects early adaptive capacity but may also be indicative of drought resilience later in the plant's life cycle. From a breeding perspective, evaluating drought tolerance at seedling-stage is rapid, operationally straightforward, and highly controllable, making it suitable for screening large germplasm collections. Multiple phenotyping approaches have been proposed for seedling-stage drought assessment. Bhattacharjee et al. (2023) reported that root length and shoot to root ratio were significantly associated with seedling-stage drought tolerance and are practical for large-scale screening. Leaf rolling reflects the ability to maintain leaf water potential under water deficit; when combined with leaf drying, it can effectively differentiate drought tolerance among varieties (Huang et al. 2022). Zu et al. (2017) developed the drought tolerance degree (DTD) , based on the proportion of green leaf length, which is simple and reliable for evaluating upland rice. Fuka et al. (1999) further showed that root development and leaf stay-green capacity jointly determine seedling survival under drought conditions. Plant height, as

an integrative indicator of overall vigor, has also been used as a morphological reference for drought evaluation (Ahmadikhah and Marufinia 2016). Nevertheless, many approaches rely on single or limited traits, which may not adequately capture the polygenic nature of drought tolerance and can compromise the comprehensiveness and accuracy of screening outcomes (Geng et al. 2024). Wei et al. (2022) assessed multiple morphological and physiological traits in 69 rice varieties and constructed an integrated index using a membership function method, thereby identifying two highly drought-tolerant varieties and supporting the utility of multi-trait evaluation.

Rice drought tolerance is governed by interconnected processes, including root development, stomatal regulation, osmotic adjustment, and signal transduction. Genome-wide association studies (GWAS) leverage natural variation and provide high mapping resolution, and have therefore become an important approach for dissecting the genetic basis of drought tolerance in rice (Huang et al. 2010). Root-related traits directly determine water acquisition efficiency and contribute substantially to drought performance. Li et al. (2017) performed GWAS on 21 root-related traits in 529 accessions, identifying 413 association signals and mapping the key drought-related gene *DRO1*; they further validated the roles of *Nal1* and *OsJAZ1* in regulating root volume and root dry weight under drought stress. Leaf rolling and stomatal movement constitute key physiological components of drought adaptation. Liu et al. (2024) performed GWAS using leaf rolling under PEG-induced stress as a core phenotype and identified *LOC_Os08g05520*, a candidate gene implicated in cell wall remodeling. Guo et al. (2018) detected 470 association loci based on 51 drought-related imaging traits in 507 accessions and functionally verified *OsPP15* as a regulator of abscisic acid (ABA)-mediated stomatal closure. Maintaining yield stability under drought remains a central breeding objective. Ghazy et al. (2024) identified 26 SNPs associated with drought-related variation

in panicle length, seed-setting rate, and panicle number in 413 accessions, and selected 22 drought-tolerant genotypes.

Integrating transcriptomic data can further refine of candidate-gene identification. Sun et al. (2022) analyzed 271 japonica accessions and proposed a Drought Resistance Index (DRI). By combining GWAS mapping, introgression-line validation, and transcriptome analysis, they identified *DROT1* and demonstrated that it enhances drought tolerance by increasing cellulose content and strengthening cell wall structure. Moreover, alternative splicing (AS) has been showned to contribute to drought-stress responses in rice (Wei et al. 2017). Yang et al. (2022b) integrated GWAS with transcriptome and AS analyses to investigate seedling-stage heat-stress responses and identified 11 key heat-responsive genes, highlighting the utility of multi-omics integration for abiotic-stress research.

Although several drought-related genes, including *OsNAC1* (Chen et al. 2023), *OsbZIP23* (Zong et al. 2016), and *OsMPK17* (Li et al. 2020), have been cloned, the genetic basis of seedling-stage drought tolerance remains incompletely understood. Many previous studies have focused on single phenotypes, lacked systematic construction of integrated drought indices, and did not sufficiently integrate transcriptomic and other functional genomics data, thereby limiting mechanistic interpretation and downstream validation. Therefore, in this study we employed a natural population of 283 *indica* rice accessions adapted to the middle and lower reaches of the Yangtze River, systematically phenotyped seedling-stage drought responses under PEG-simulated drought stress, developed a multi-trait integrated index, and screened representative drought-tolerant germplasm. We further combined GWAS with RNA sequencing (RNA-seq) analysis to identify candidate genes associated with seedling-stage drought tolerance and to explore their

putative regulatory mechanisms, aiming to provide a foundation for future breeding improvement in rice.

Material and Methods

Plant Materials and Drought Stress Treatment

A natrual population of 283 *indica* rice accessions was used in this study. These accessions capture broad genetic diversity originating from South and Southeast Asia, including China, the Philippines, and India, with a subset carring partial *japonica* ancestry. All germplasm materials were provided by the Hubei Academy of Agricultural Sciences.

Seeds were dried at 45℃ for 7 d to break dormancy, surface-sterilized in 2 g L^{-1} sodium hypochlorite for 4 h, and thoroughly rinsed with distilled water. Seeds were then germinated at 30 °C for 3 d, and uniformly germinated seeds were selected and sown in 96-well plates with perforated bottoms. The plates were placed in hydroponic containers and cultivated in a growth chamber under the following conditions: 28 °C (light) / 26 °C (dark), 16 h/8 h light/dark photoperiod, 200 μmol m^{-2} s^{-1} light intensity, and 70% relative humidity. Seedlings were grown in Yoshida nutrient solution (Yoshida et al. 1971), which was renewed every 2 d to maintain nutrient stability.

After 14 d of growth, seedlings were divided into a control group (CK) and a drought-stress treatment group (TR). The CK group continued to receive standard Yoshida solution, whereas the TR group was exposed to Yoshida solution supplemented with 20% (w/v) PEG6000 to impose osmotic stress. Following 7 d of stress treatment and 3 d of rewatering, the maximum root length (RL, cm), plant height (PH, cm), leaf senescence resistance index (LSRI), and leaf wilting score

144 (LW) were recorded for each accession.

145 **Measurement and Calculation of Drought Tolerance Indices**

146 For each accession, three seedlings were sampled from both the control and drought treatment
147 groups. After washing, PH and RL were measured, and the drought resistance coefficient (DRC)
148 was calculated according to Eq. (1). The DRC of plant height (DPH) and the DRC of root length
149 (DRL) were used in subsequent analyses. Leaf wilting was visually scored according to the criteria
150 detailed in Table S1. Leaf senescence resistance was quantified using LSRI. For each seedling, the
151 total leaf length and the green segment length from the leaf base to the necrotic boundary) were
152 measured for all fully expanded leaves. The mean total leaf length and mean green segment length
153 across leaves were then calculated, and LSRI was defined as the ratio of the mean green segment
154 length to the mean total leaf length.

155 $$DRC = TR/CK \quad (1)$$

156 Following the method of Li et al. (Li et al. 2015), a comprehensive drought tolerance metric
157 (CDTM) was constructed to evaluate and rank the drought tolerance of all accessions. To reduce
158 bias from single-trait evaluation, fuzzy membership function analysis was applied to four traits. For
159 positively associated traits (RL, PH, and LSRI), membership values were calculated using Eq. (2);
160 for RL and PH, DRC values were used. For the negatively associated trait (LW), Eq. (3) was applied:

161 $$\mu(X_i) = (X_i - X_{min})/(X_{max} - X_{min}) \quad i = 1,2,3,\dots n \quad (2)$$

162 $$\mu(X_i) = 1 - (X_i - X_{min})/(X_{max} - X_{min}) \quad i = 1,2,3,\dots n \quad (3)$$

163 Where $\mu(X_i)$ is the membership value for accession i, X_i is the observed trait value, and
164 X_{min} and X_{max} are the minimum and maximum values of the trait across accessions, respectively.

Trait weights were calculated using Eq. (4):

$$W_j = \sigma_j / \sum_{j=1}^{n} \overline{X_j} \quad j = 1,2,3,\ldots n \tag{4}$$

where W_j is the weight coefficient of trait j, σ_j is the standard deviation, and $\overline{X_j}$ is the mean value of trait j. CDTM was calculated using Eq. (5):

$$CDTM = \sum_{i=1}^{n} \left(\mu(X_i) \cdot W_j\right) \quad i = 1,2,3,\ldots n; j = 1,2,3,\ldots n \tag{5}$$

Higher CDTM values indicate stronger drought tolerance under TR conditions.

Based on CDTM values, drought tolerance of the 283 accessions was evaluated using both hierarchical clustering and stepwise classification method, and the two approaches were jointly used to identify drought-tolerant and drought-sensitive materials at the seedling stage. For hierarchical clustering, the factoextra package in R was used to determine the optimal number of clusters (fviz_nbclust). Euclidean distances were calculated with dist function, and clustering was performed with hclust using Ward's linkage method. In addition, accessions were categorized into five drought-tolerance categories based on CDTM according to the stepwise classification method described by Lu et al. (2005). In the first step, all accessions were divided into three categories based on the overall mean (Mean) and standard deviation (SD) of CDTM values: highly drought-tolerant($CDTM \geq Mean + SD$), , intermediate ($Mean - SD \leq CDTM \leq Mean + SD$), and highly drought-sensitive ($CDTM \leq Mean - SD$). In the second step, the intermediate group was further subdivided using its own mean ($Mean_{mid}$) and standard deviation (SD_{mid}) into three subgroups: drought-tolerant($CDTM \geq Mean_{mid} + SD_{mid}$), moderately drought-tolerant($Mean_{mid} - SD_{mid} \leq CDTM \leq Mean_{mid} + SD_{mid}$), and drought-sensitive($CDTM \leq Mean_{mid} + SD_{mid}$). Ultimately, all accessions were classified into five drought tolerance categories: highly drought-tolerant, drought-tolerant, moderately drought-tolerant, drought-sensitive, and highly drought-sensitive.

Redox status Analysis

Based on CDTM rankings, the drought-tolerant cultivar *Jiangnongzao 1B* (DT) and the

drought-sensitive cultivar *TAISEN GLUTINOUS YU 1157* (DS), were selected for redox-status characterization. Seedlings were grown in standard Yoshida nutrient solution for 14 d and then subjected to osmotic stress using Yoshida solution supplemented with 20% (w/v) PEG6000. Fresh leaf samples were collected at 0 d (control), 3 d, and 7 d after stress initiation. The activities of superoxide dismutase (SOD) and peroxidase (POD), as well as the contents of malondialdehyde (MDA) and hydrogen peroxide (H_2O_2), were determined using commercial assay kits (Solarbio, Beijing, China) following the manufacturer's instructions. Each treatment included three biological replicates.

Resequencing and Genotyping

Genomic DNA was extracted from young rice leaf tissues. The DNA was fragmented to approximately 500 bp using a Covaris S2. NEBNext DNA Library Prep Reagent Set for Illumina (BioLabs) constructs the DNA library. Library was sequenced on the Illumina HiSeq X10 platform using paired-end sequencing, achieving a sequencing depth of 11×. The reads were aligned to the Nipponbare reference genome (IRGSP-1.0) using BWA (Li and Durbin 2009). SNP calling was performed using the GATK (McKenna et al. 2010). To ensure genotyping accuracy, SNPs with > 20% missing data were removed; heterozygous sites were treated as missing and imputed using NPUTE (Roberts et al. 2007) ; and SNPs with a minor allele frequency (MAF) < 0.05 were excluded. A total of 2,348,117 high-quality SNPs were retained for subsequent GWAS.

Population Structure and Linkage Disequilibrium Analysis

Population structure was inferred using ADMIXTURE (Alexander et al. 2009) based on maximum likelihood estimation , with the number of ancestral populations (K) ranging from 1 to

20. A PHYLIP file was selected using the vcf2phylip script (https://github.com/edgardomortiz/vcf2phylip/), and a phylogenetic tree was constructed using the neighbor-joining method implemented in MEGA-X (Tamura et al. 2021). Principal component analysis (PCA) was performed using PLINK version 1.9 (Purcell et al. 2007). Genome-wide linkage disequilibrium (LD) decay was estimated using PopLDdecay (Zhang et al. 2019a), and the LD decay distance was defined as the physical distance (kb) at which the r^2 value decreased to 50% of its maximum.

Genome-Wide Association Analysis

GWAS was performed using six multi-locus models, including mrMLM, FASTmrMLM, FASTmrEMMA, pLARmEB, pKWmEB, and ISIS EM-BLASSO, implemented in the mrMLM software (Zhang et al. 2020). The analyzed traits included DRL , DPH, LSRI, LW, and CDTM. Significant associations were determined using thresholds of -log10(*P*-value) > 3 and LOD > 3, as recommended by Zhang et al. (2019b), to balance detection power and false-positive control. Candidate genes located within ± 50 kb of each significant SNP were annotated based on gene annotation information obtained from the China National Rice Data Center (https://www.ricedata.cn/gene/). Manhattan and Q-Q plots were generated using the CMplot package in R.

RNA Sequencing and Data Analysis

RNA sequencing was performed for DT and DS under control and drought-stress conditions. Drought stress was simulated by replacing standard Yoshida solution with solution containing 20% (w/v) PEG6000 and maintained for 24 h. Leaf samples were collected at 0 h and 24 h. For each time

point, three uniformly growing seedlings were randomly selected per replicate, and leaf tissues were immediately frozen in liquid nitrogen and stored at −80 °C. Three biological replicates were included for each treatment. RNA extraction, quality assessment, library construction, and sequencing were performed by Genedenovo Biotechnology Co., Ltd. (Guangzhou, China).

Clean reads were aligned to the Nipponbare reference genome (IRGSP-1.0) using HISAT2(Kim et al. 2015) with the parameter setting“rna-strandness RF” ; other parameters were kept as default. Gene expression levels were normalized using transcripts per million (TPM) (Zhao et al. 2020). Differential expression analysis was performed using the R package DESeq2 (Love et al. 2014) based on read counts, with thresholds of $|\log_2 FC| > 1$ and adjusted *P*-value < 0.05. Significantly differentially expressed genes (DEGs) were subjected to Gene Ontology (GO) and Kyoto Encyclopedia of Genes and Genomes (KEGG) enrichment analyses. All analyses were conducted on the Omicsmart platform (https://www.omicsmart.com/).

Alternative Splicing Analysis

Alternative splicing events were identified using rMATS (Shen et al. 2014), including skipped exon (SE), retained intron (RI), alternative 5’splice sites (A5SS), alternative 3’splice sites (A3SS), and mutually exclusive exons (MXE). Differential alternative splicing (DAS) events among comparison groups were considered significant at false discovery rate (FDR) < 0.05. Genes harboring significant SE or RI events were defined as differentially spliced genes. All analyses were conducted on the Omicsmart platform (https://www.omicsmart.com/).

Integrated GWAS and Transcriptome Analysis

To prioritize putative functional genes, we intersected the GWAS-derived candidate genes with

DEGs, yielding a set of genes supported by both genetic association signals and transcriptional responses to drought. The frequency of these genes across different drought-related traits was further summarized. For further validation, public RNA-seq data from drought-stressed seedlings of the water-saving and drought-resistant variety *Hanyou 73* (*HY73*) were retrieved from the NCBI SRA database (BioProject: PRJNA790757). These data were processed using the same pipeline described above, followed by differential expression analysis and cross-validation with the prioritized gene set. In parallel, AS analysis was performed using rMATS, and differentially spliced genes were overlapped with the integrated candidate gene list.

Result

Phenotypic Analysis of Seedling-Stage Drought Tolerance

PH, RL, LSRI, and LW were measured in 283 *indica* rice accessions under control (CK) and drought treatment (TR) conditions (Table S2,S3). Drought stress significantly inhibited shoot growth, with the average PH decreasing from 33.3 cm under CK to 26.4 cm under TR, and 96.5% of the accessions (273/283) showing varying degrees of height reduction (Fig. 1A). In contrast, RL showed a slight increase under drought stress, with the mean value rising from 12.2 cm to 13.3 cm, suggesting that some accessions may enhance water uptake through root elongation (Fig. 1B).The mean values of the LSRI and LW were 66.1% and 2.6, with coefficients of variation of 27.61% and 37.02%, respectively, indicating substantial variation in leaf physiological responses among accessions under drought stress. Accessions exhibiting higher LSRI and lower LW showed stronger drought adaptability, which may be associated with differences in osmotic adjustment, antioxidant capacity, and photosynthetic protection.

Based on DPH, DRL, LSRI and LW, CDTM was constructed to integratively evaluate drought tolerance across accessions. Correlation analysis revealed a highly significant negative correlation between LSRI and LW (r = −0.78, $p < 0.001$). LSRI was significantly positively correlated with DPH, DRL, and CDTM, with DRL showing the strongest correlation with CDTM (r = 0.72, $p < 0.001$), suggesting a dominant role of root development in seedling-stage drought tolerance (Fig. 1C). Phenotypic distribution analysis indicated that DPH, DRL, and CDTM were approximately normally distributed, whereas LSRI and LW were skewed, consistent with the genetic characteristics of quantitative traits (Fig. S1).

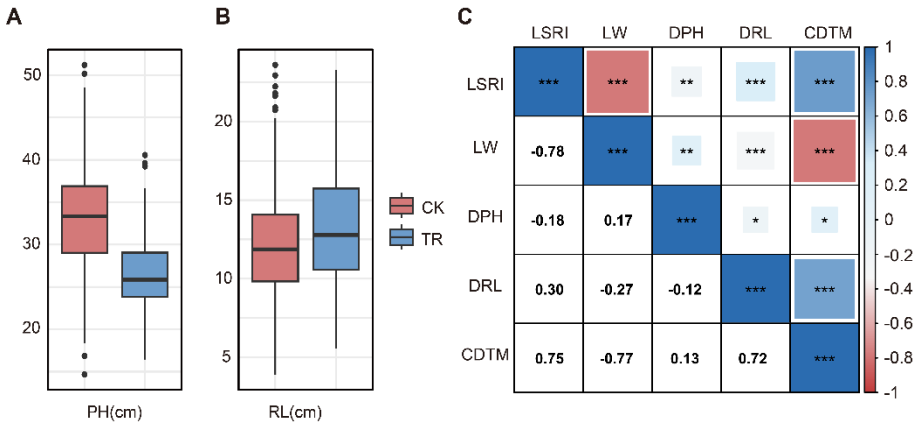


Figure.1 Drought tolerance-related phenotypes. (**A**) Plant height under control (CK) and drought treatment (TR) conditions. (**B**) Root length under CK and TR. (**C**) Correlation analysis among five drought-related traits. Correlations were calculated using Pearson's correlation coefficient. *, P < 0.05; **, P < 0.01; ***, P < 0.001. LSRI, leaf senescence resistance index; LW, leaf wilting score; DPH, DRC of plant height; DRL, DRC of root length; CDTM, comprehensive drought tolerance metric.

Evaluation of Drought Tolerance

Hierarchical clustering analysis based on CDTM divided the 283 accessions into six major groups. (Fig. 2B, S2; Table S3). Group I comprised 10 accessions (3.53%) with CDTM values ranging from 0.7203 to 0.8446 and LW predominantly at grade 1, indicating minimal plant growth

294 impairment under drought stress; this group was classified as extremely drought-tolerant. Group II
295 included 40 accessions (14.13%) with CDTM values of 0.6166 – 0.7061 and LW mainly at grades
296 1 – 2, classified as strongly drought-tolerant. Group III consisted of 68 accessions (24.03%) with
297 CDTM values ranging from 0.5217 to 0.6118 and LW primarily at grade 2, classified as moderately
298 drought-tolerant. Groups IV and V comprised 83 and 67 accessions (29.33% and 23.67%),
299 respectively, with CDTM values of 0.4315 – 0.5188 and 0.3157 – 0.4284, and LW mainly at grades
300 2 – 3 and grade 3, classified as mildly drought-tolerant and weakly drought-tolerant, respectively.
301 Group VI contained 15 accessions (5.30%) with CDTM values of 0.1195 – 0.2895, and LW
302 concentrated at grades 4 – 5, with some seedlings completely desiccated; this group was classified
303 as extremely drought-sensitive.

304 To validate the clustering results, a stepwise classification method was applied using CDTM
305 as the evaluation index. The 283 accessions were further classified into five drought tolerance
306 categories: highly drought-tolerant (CDTM $\geqslant$ 0.624; 49 accessions, 17.31%), drought-tolerant
307 (0.558 $\leqslant$ CDTM < 0.624; 41 accessions, 14.49%), moderately drought-tolerant (0.427 $\leqslant$
308 CDTM < 0.558; 113 accessions, 39.93%), drought-sensitive (0.374 $\leqslant$ CDTM < 0.427; 40
309 accessions, 14.13%), and highly drought-sensitive (CDTM $\leqslant$ 0.374; 40 accessions, 14.13%)
310 (Table S4). The classification from hierarchical clustering and stepwise classification were highly
311 consistent. Based on the integrated results, 10 accessions were ultimately identified as extremely
312 drought-tolerant at the seedling stage (Table S5).

313 The extremely drought-tolerant cultivar *Jiangnongzao 1B* (DT) and the extremely drought-
314 sensitive cultivar *TAISEN GLUTINOUS YU 1157* (DS) were selected for phenotypic and
315 physiological comparison under 20% (w/v) PEG-induced drought stress. After 7 d of PEG treatment,

DS plants exhibited severe leaf rolling and wilting, with partial leaf tip chlorosis, whereas DT plants showed only mild leaf curling and maintained overall normal morphology, indicating stronger drought tolerance (Fig. 2A).

Physiological measurements were consistent with phenotypic observations. SOD and POD activities and MDA and H_2O_2 contents were quantified at 0, 3, and 7 d after drought treatment. POD activity and MDA content differed significantly between the two cultivars (Fig. 2C, D), whereas SOD activity and H_2O_2 content did not (Fig. S3). Under control conditions, POD activity was comparable between the two cultivars. After 3 d of drought stress, POD activity increased by 5.7% in DT but decreased by 7.3% in DS. After 7 d, POD activity in DT was 25.6% higher than the control, significantly exceeding that in DS (Fig. 2C). Conversely, MDA content showed an opposite trend (Fig. 2D). Although MDA levels were similar between cultivars under control and 3 d stress conditions, by 7 d the increase in DS (54.1%) significantly exceeded that in DT (32.2%). These results suggest that DT maintains higher antioxidant capacity and reduced lipid peroxidation under drought, supporting the CDTM-based classification.

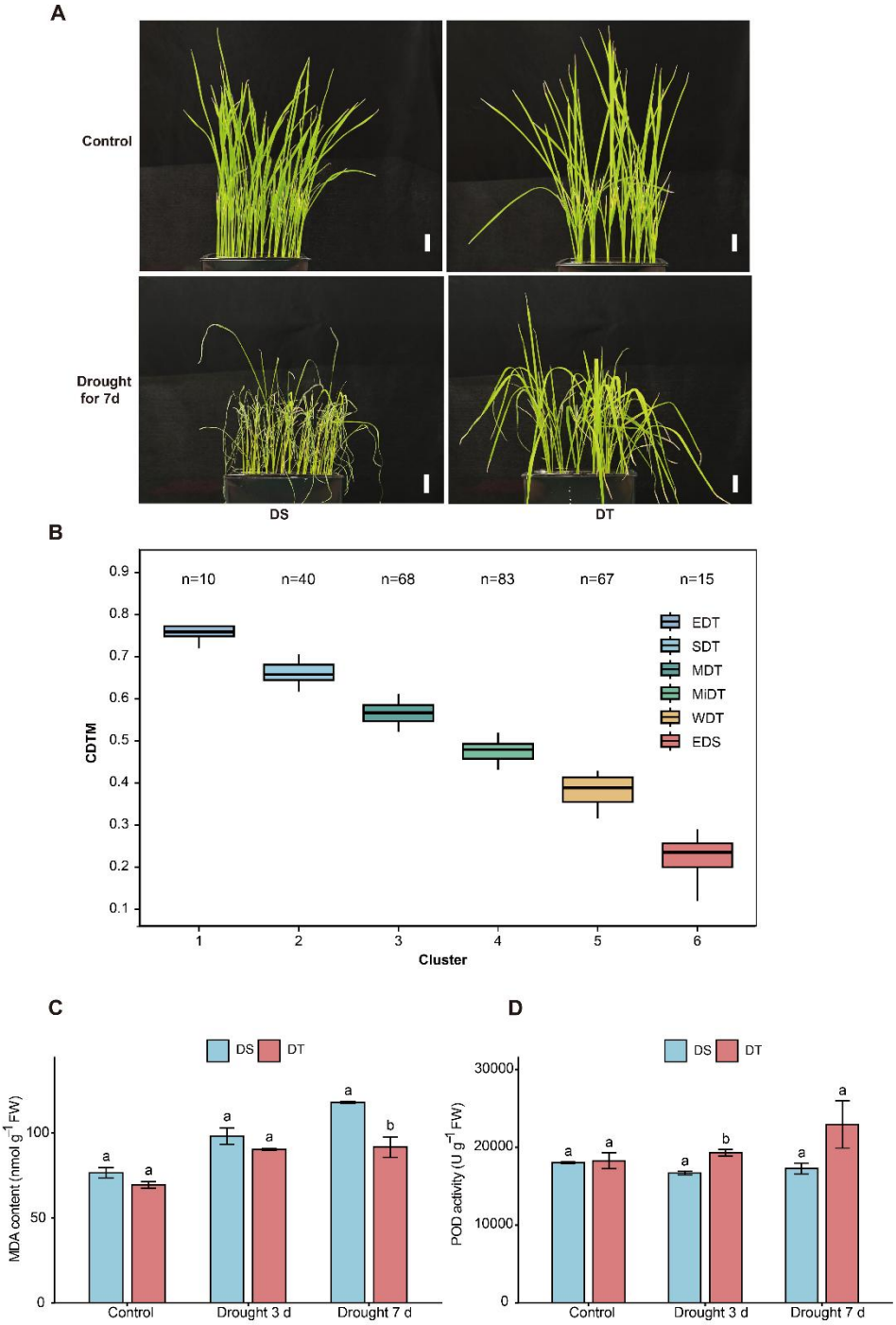
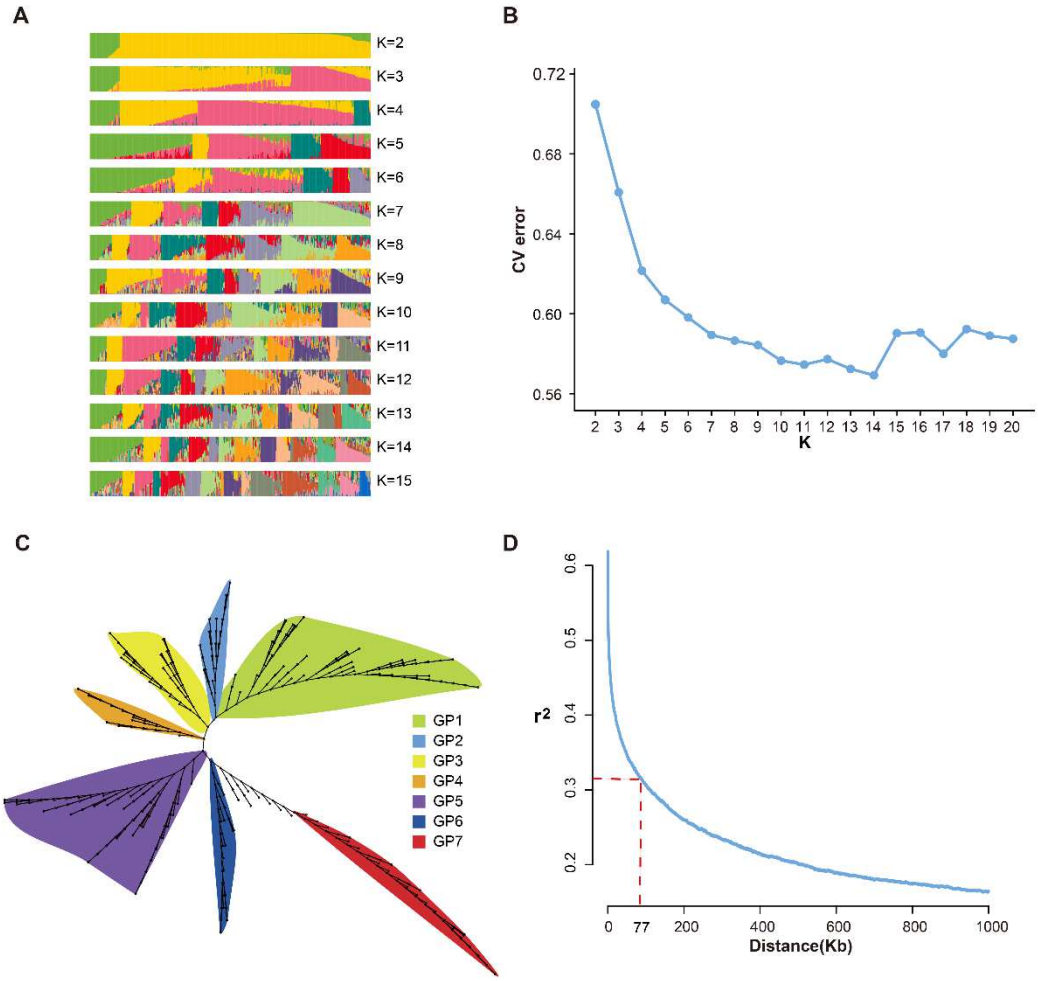


Figure.2 Classification of seedling-stage drought tolerance. (**A**) Phenotypic performance of DS and DT under 20% (w/v) PEG6000 treatment. Scale bars = 2 cm. (**B**) Hierarchical cluster analysis of 283 *indica* rice accessions based on CDTM. Accessions were classified into six drought tolerance grades (EDT to EDS). Boxplots show the CDTM distribution for each grade, with the number of accessions indicated above. (**C**) POD activity. (**D**) MDA content. Samples were collected at 0 d (control), 3 d, and 7 d after 20% PEG treatment. Data are presented as mean ± SE (n = 3). Different letters indicate significant differences among cultivars at the same time point (Student's t-

test, $P < 0.05$). EDT, extremely drought-tolerant; SDT, strongly drought-tolerant; MDT, moderately drought-tolerant; MiDT, mildly drought-tolerant; WDT, weakly drought-tolerant; EDS, extremely drought-sensitive.

Population Structure and Linkage Disequilibrium Analysis

The structure bar plot (Fig. 3A) illustrates the genetic components of each accession under different K values, with progressively clearer stratification as K increased. K values ranging from 2 to 20 were evaluated, and the optimal grouping was determined based on the CV error. The CV error decreased more slowly at K = 7 and showed a slight increase when K > 14 (Fig. 3B); therefore, K = 7 was selected for subsequent population classification. The phylogenetic tree also supported the division of the population into seven major subgroups (GP1–GP7) (Fig. 3C). Based on the classfication reported by Wang et al. from the 3K Rice Genome Project (Wang et al. 2018), GP1 mainly comprised East Asian *indica* accessions from China; GP2 and GP4 contained mixed genetic backgrounds, mainly from China and the Philippines, respectively; GP3 included modern cultivated *indica* accessions from multiple origins; GP5 consisted primarily of *indica* accessions from India and South Asia; GP6 corresponded primarily to the *Aus* group; and GP7 showed evident japonica ancestry. PCA indicated that the first eight principal components explained 81.65% of the total variance, with PC1 and PC2 accounting for 47% and 11%, respectively (Fig. S4). LD decay analysis showed that r^2 declined to half of its maximum at an inter-marker distance of approximately 77 kb, indicating an LD decay distance of ~77 kb in this population (Fig. 3D). Collectively, these results suggest substantial genetic diversity and moderate population differentiation, providing a reliable genetic basis for subsequent GWAS.



359 **Fig. 3** Population structure and linkage disequilibrium (LD) decay in 283 rice accessions. (**A**)
360 Population structure bar plot. (**B**) Cross-validation (CV) error for K = 1 – 20. (**C**) Phylogenetic tree.
361 (**D**) LD decay in the 283 accessions. The red dashed line denotes the physical distance at which r^2
362 drops to half of its maximum.

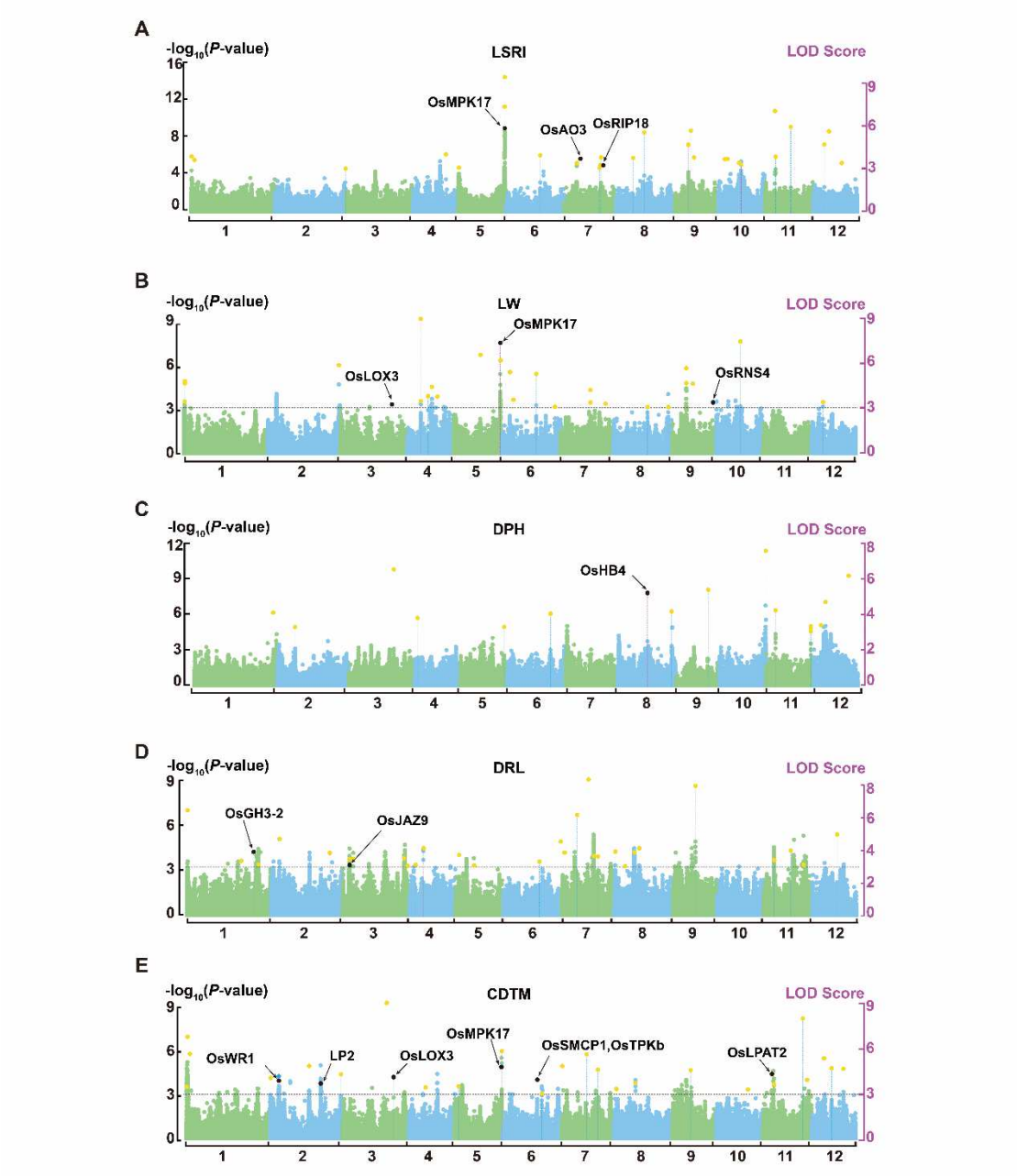
363 **GWAS Identifies Genetic Loci Significantly Associated with Seedling-Stage Drought**
364 **Tolerance**

365 Based on the mrMLM multi-locus framework, GWAS was performed for five drought-related
366 traits, including DPH, DRL, LSRI, LW, and CDTM (Fig. 4A-E, S5). A total of 138 significant SNPs
367 were identified across all 12 chromosomes (Table S6). Specifically, 30, 28, 17, 32, and 31 SNPs
368 were detected for the five traits, respectively. Among these, eight SNPs were associated with more
369 than one trait (Table S7), suggesting potential pleiotropy and coordinated genetic control under

drought stress. Significant signals were unevenly distributed across the genome, with chromosome 7 harboring the most loci (17) and chromosome 10 the fewest (7).

In total, 133 candidate genes were annotated within ± 50 kb of each significant SNP, including 13 previously reported drought-related genes and 22 genes detected across multiple traits. Specifically, 27, 29, 26, 40, and 39 candidate genes were associated with LSRI, LW, DPH, DRL, and CDTM (Tables S8-S12), respectively. Notably, CDTM was linked to a larger set of previously reported drought-related genes than any single trait, supporting its ability to integrate drought-relevant genetic information. In addition, several candidate genes were repeatedly identified across multiple traits. For example, *OsLOX3* was detected in association with both LW and CDTM, while *OsMPK17* was simultaneously associated with LSRI, LW, and CDTM.

Functional annotation indicated that the previously reported drought-related genes were mainly involved in ABA and jasmonic acid (JA) metabolism and signaling, mitogen-activated protein kinase (MAPK) cascade pathways, transcriptional regulation, lipid metabolism, and protein homeostasis.

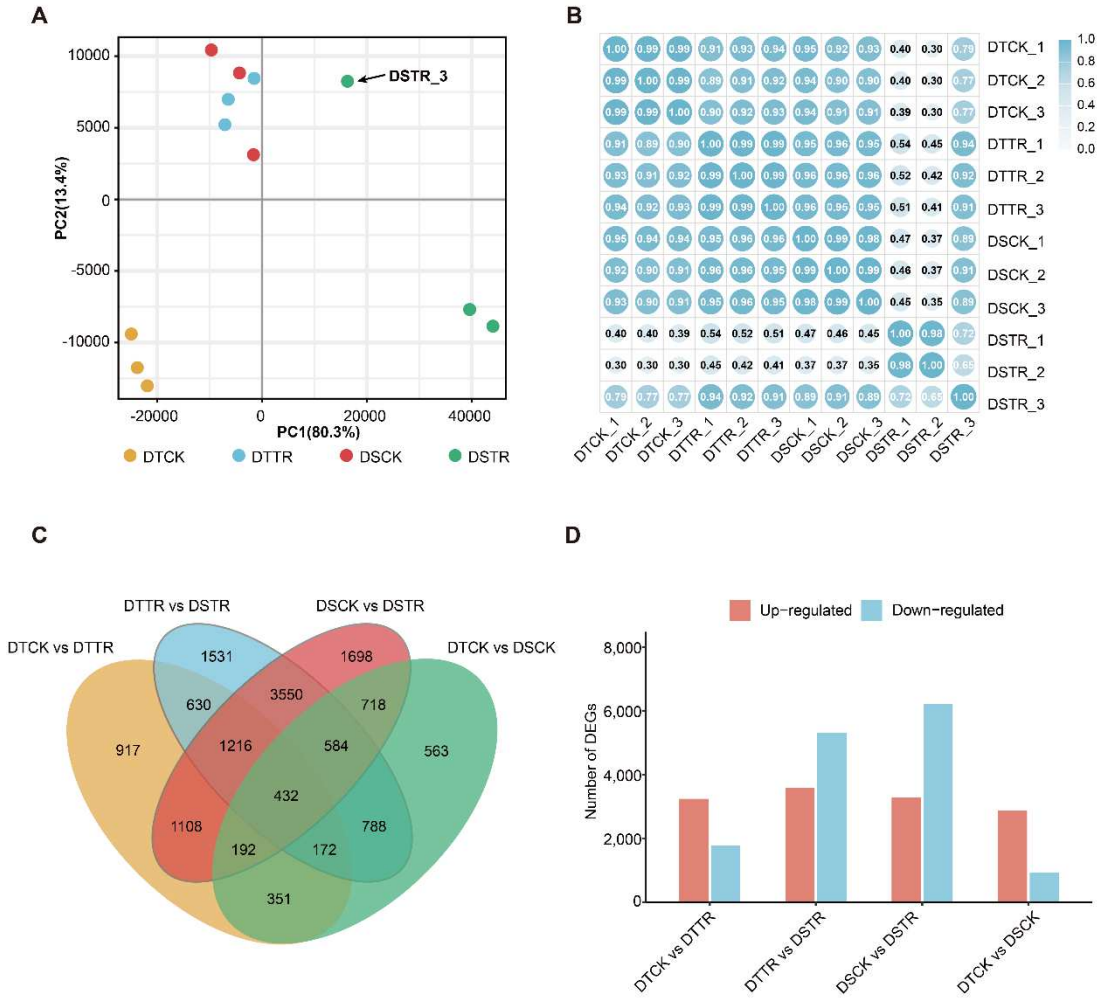


384 **Figure.4** Genome-wide association analysis of five drought-related traits at the seedling stage in
385 rice. (**A**) Leaf senescence resistance index. (**B**) Leaf wilting score. (**C**) DRC of plant height. (**D**)
386 DRC of root length. (**E**) CDTM. The dashed horizontal line indicates the significance threshold
387 (LOD = 3). Yellow dots represent significantly associated SNPs, and black labels denote candidate
388 genes previously implicated in drought tolerance.

389 **Differentially Expressed Genes in Response to Drought Stress**

RNA-seq was performed for DT and DS under control and drought treatment conditions. PCA showed that biological replicates of DTCK, DTTR, and DSCK clustered tightly, whereas DSTR_3 was clearly separated from DSTR_1 and DSTR_2 (Fig. 5A). Pearson correlation analysis further confirmed that, with the exception of the DSTR group, correlation coefficients among replicates within all other treatment groups exceeded 0.987, whereas DSTR_3 showed relatively low correlations with DSTR_1 (0.726) and DSTR_2 (0.652) (Fig. 5B), indicating high overall reproducibility of the remaining samples. Based on the combined PCA and correlation analyses, DSTR_3 was identified as an outlier and excluded from subsequent analyses to ensure data accuracy and consistency.

Comparative transcriptomic analyses between DT and DS under different treatment conditions identified a total of 14,450 differentially expressed genes (DEGs) (Fig. 5C, D). In the DTCK vs DTTR comparison, 5,018 DEGs were detected, including 3,243 upregulated and 1,775 downregulated genes. In contrast, the DSCK vs DSTR comparison yielded 9,498 DEGs, comprising 3,283 upregulated and 6,215 downregulated genes, with the number of downregulated genes substantially exceeding that of upregulated genes. This pattern indicates broader transcriptional repression in the drought-sensitive cultivar under drought stress. In cultivar comparisons under drought conditions (DTTR vs DSTR), 8,903 DEGs were identified, of which 1,531 were unique to this comparison and not detected in other contrasts, indicating marked divergence in drought-responsive transcriptional programs between the tolerant and sensitive cultivars. Under non-stress conditions (DTCK vs DSCK), 3,800 DEGs were detected, including 563 uniquely expressed genes, reflecting inherent differences in basal metabolism and homeostatic regulation between the two cultivars.



412 **Figure 5** Transcriptomic responses of DT and DS under drought stress. (**A**) Principal component
413 analysis based on gene expression profiles. (**B**) Pairwise Pearson correlation coefficients among
414 samples based on normalized gene expression, shown as a correlogram. (**C**) Venn diagram
415 illustrating the overlap of differentially expressed genes among the four pairwise comparisons. (**D**)
416 Distribution of the numbers of DEGs in each comparison. DTCK and DSCK represent control
417 samples of DT and DS, respectively, whereas DTTR and DSTR represent drought-treated samples.
418 Numbers 1-3 indicate biological replicates.

419 **GO and KEGG Enrichment Analyses of Drought Responsive DEGs**

420 All 14,450 DEGs were subjected to GO and KEGG enrichment analyses. GO enrichment
421 analysis showed that DEGs were mainly enriched in biological process (BP), molecular function
422 (MF), and cellular component (CC) categories. A total of 50 level-2 GO terms were enriched in

both DTCK vs DTTR and DSCK vs DSTR, with BP and MF terms far outnumbering CC terms (only three).

Further analysis of the top 10 enriched GO terms revealed cultivar-dependent functional signatures (Fig. 6). In BP, both DT and DS were enriched for organic acid metabolism, oxoacid metabolism, and small-molecule metabolism, whereas catalytic activity and oxidoreductase activity were shared MF terms. In DS, DEGs were specifically enriched for small-molecule biosynthetic processes, and the enriched CC terms were mainly associated with the chloroplast and thylakoid-related components (Fig. 6A). In contrast, DT showed specific enrichment in small-molecule catabolic processes, monocarboxylic acid metabolism, and organic acid biosynthesis (Fig. 6B).

KEGG pathway analysis further highlighted marked differences in molecular response mechanisms between the two cultivars. In DT, DEGs were significantly enriched in fatty acid degradation, branched-chain amino acid degradation, α-linolenic acid metabolism, pyruvate metabolism, and peroxisome (Fig. S6A). These pathways are closely associated with energy metabolism, membrane lipid remodeling, and reactive oxygen species (ROS) scavenging, among which α-linolenic acid metabolism is upstream of JA biosynthesis (Wasternack and Song 2016). In contrast, DS showed specific enrichment in photosynthesis, carbon metabolism, glutathione metabolism, and plant hormone signal transduction (Fig. S6B). Glutathione metabolism is involved in ROS detoxification (Dorion et al. 2021), and enrichment of hormone signaling pathways suggests

that DS may rely more on hormone-mediated responses under drought stress.

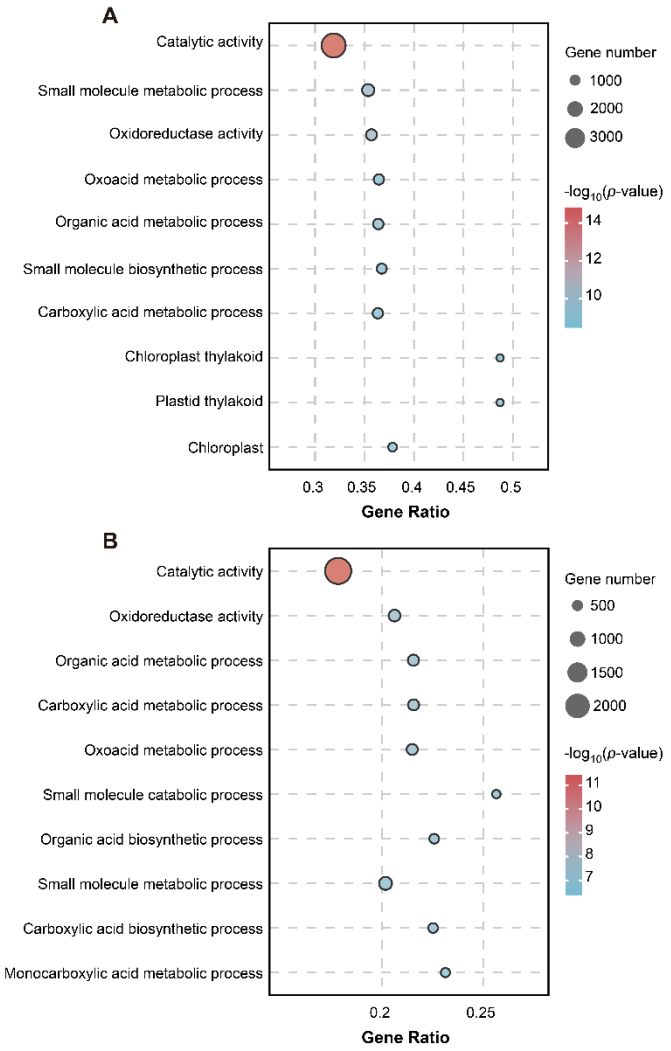


Figure.6 GO enrichment analysis of DEGs. (**A**) DS; (**B**) DT. The top 10 significantly enriched GO terms are shown.

Alternative Splicing Profiling under Drought Stress

Five typical AS types were identified, including skipped exon, retained intron, alternative 5’ splice sites, alternative 3’splice sites, and mutually exclusive exons (Fig. 7A). Approximately 16,000 AS events were detected across the four sample groups, with SE accounting for the largest proportion (7,132 – 9,588 events), representing 53% – 60% of all events. RI events accounted for 18% – 22%, A3SS and A5SS for 11% – 14% and 6% – 8%, respectively, whereas MXE represented

the smallest proportion (3% – 4%). Overall, the composition of AS types was largely consistent across cultivars and treatments.

Differential alternative splicing analysis was conducted for DTCK vs DTTR, DSCK vs DSTR, DTCK vs DSCK, and DTTR vs DSTR comparisons, yielding 4,436, 6,395, 4,657, and 6,503 significant events, respectively (FDR < 0.05; Fig. 7B). Among these, SE and RI accounted for a relatively high proportion, suggesting that drought stress is accompanied by widespread changes in splicing patterns at the seedling stage, with cultivar-dependent differences between drought-tolerant and drought-sensitive backgrounds.

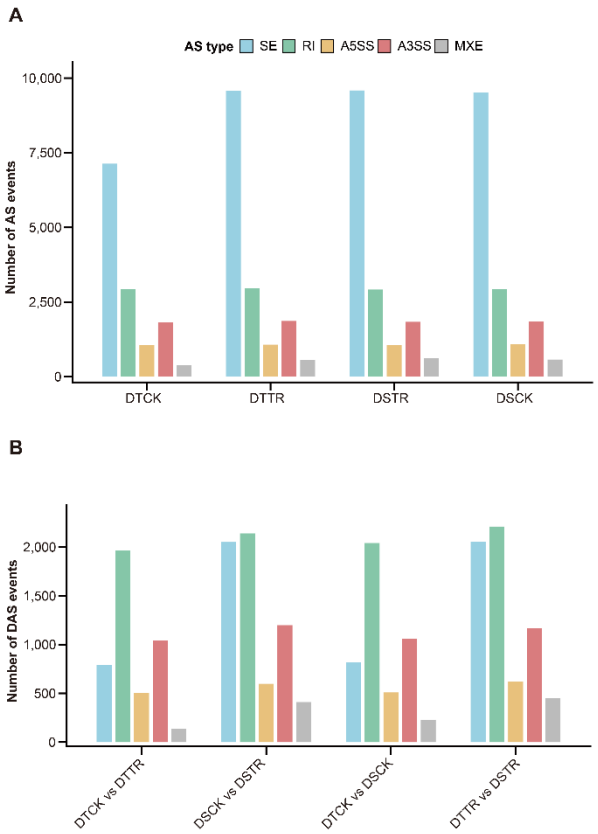


Fig.7. Alternative splicing analysis under drought stress at the rice seedling stage. (**A**) Numbers of five AS event types in the four sample groups, including skipped exon (SE), retained intron (RI), alternative 5’ splice site (A5SS), alternative 3’ splice site (A3SS), and mutually exclusive exons (MXE). (**B**) Numbers of significant differential AS events across the indicated comparisons.

Integrative Analysis Identifies Key Candidate Genes involved in Drought Response

To systematically identify key functional genes associated with drought tolerance, we integrated GWAS results with transcriptomic analyses. GWAS identified 133 candidate genes significantly associated with drought-related traits. Integration with RNA-seq data showed that 69 genes (51.9%) were differentially expressed under drought stress, indicating that approximately half of the GWAS-identified candidate genes displayed drought-responsive transcriptional changes. Notably, 12 genes were repeatedly detected across multiple drought-related traits (Table S13).

To validate the expression patterns of these candidate genes in an independent drought-resistant cultivar, public RNA-seq data from drought-stressed seedlings of the water-saving and drought-resistant rice variety *Hanyou 73* were retrieved for cross-validation. Six of the twelve candidate genes also showed significant differential expression in *HY73*, including *Os01g0110100* (*OsPHO1-1*), *Os02g0817600* (*OsIAA10*), *Os02g0817900* (*CYP97A4*), *Os02g0818000* (*OsCBSX3*), *Os05g0576800* (*OsMPK17*), and *Os05g0580000* (*OsAGPL1*). Based on their expression patterns, these six genes were grouped into three response categories (Fig. 8A, S7). *Os05g0580000* was consistently upregulated in DS, DT, and *HY73*, indicating a stable drought-inducible expression pattern, whereas *Os02g0817600* and *Os05g0576800* were consistently downregulated in all three cultivars. In contrast, *Os01g0110100, Os02g0817900*, and *Os02g0818000* displayed pronounced cultivar-specific expression patterns, with opposite expression trends between drought-tolerant and drought-sensitive cultivars, which may reflect divergent regulatory responses across genetic backgrounds. Functional annotation indicated that these genes are involved in phosphate transport,

auxin signaling, carotenoid metabolism, sulfur-related processes, MAPK signaling, and starch biosynthesis.

Although RI is often reported as a prevalent AS type in plants, Yang et al. (2022a) reported that SE may play a more prominent role in rice responses to drought. Accordingly, we identified differential AS events under drought stress using rMATS and intersected genes carrying significant SE or RI events with the GWAS-RNA-seq integrated candidate set, ultimately identifying *Os03g0700700* (*OsLOX1*) as a key differentially spliced gene. *Os03g0700700* showed a significant SE event in both DSCK vs DSTR and DTTR vs DSTR, and the SE event in DSCK vs DSTR mapped to Chr3: 28,111,157–28,111,506 (Fig. 8B). These results suggest that drought stress may alter isoform composition via exon skipping, potentially affecting protein function.*OsLOX1* encodes a lipoxygenase (*LOX*), a key enzyme in the oxylipin signaling pathway involved in lipid peroxidation and the initial steps of JA biosynthesis (Hou et al. 2016). These findings provide prioritized targets for downstream functional validation and breeding for drought resilience.

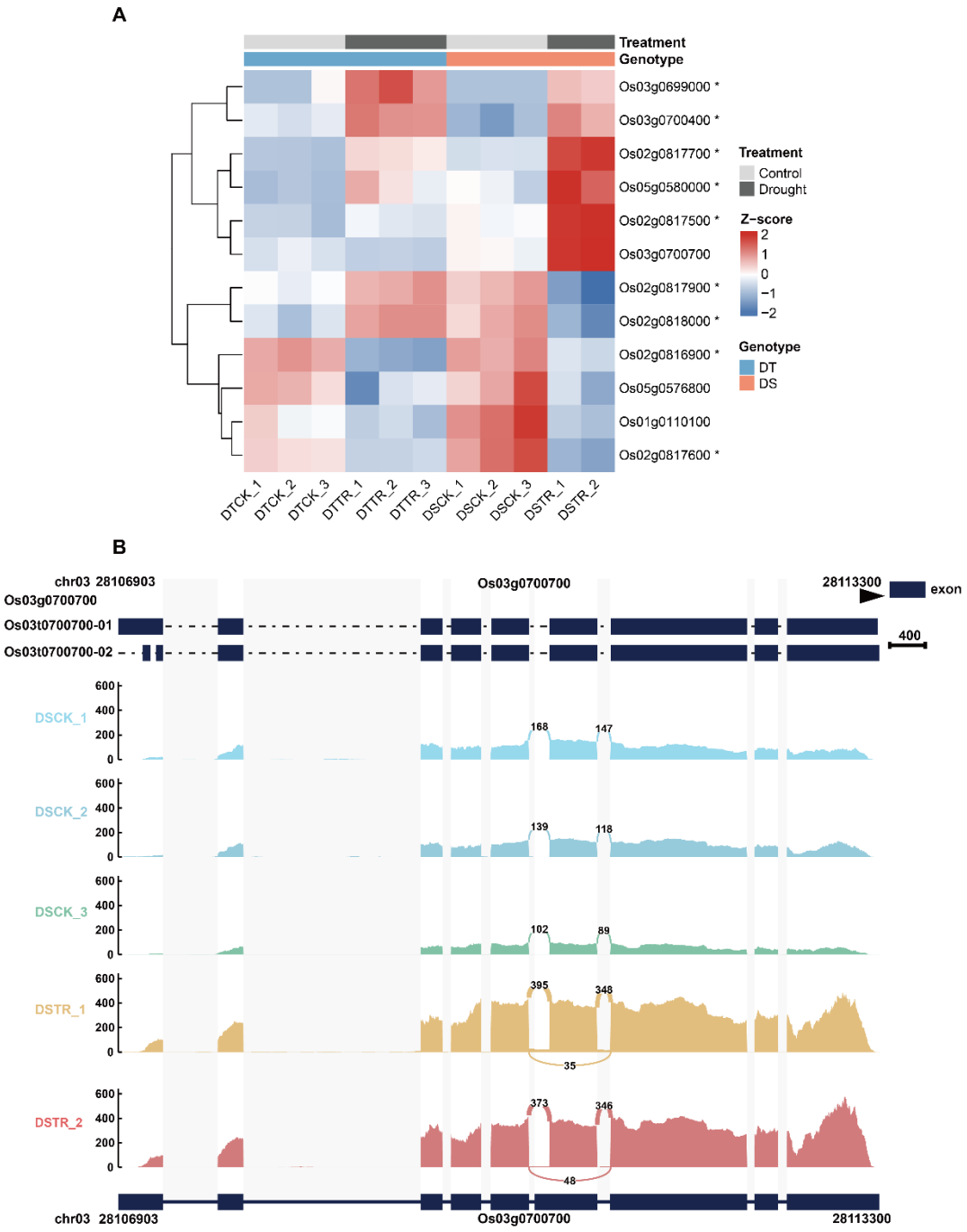


Fig.8 Screening of drought-related candidate genes. (**A**) Heatmap showing the expression profiles of 12 candidate genes in DT and DS under control and drought treatment condition. Expression values were transformed using the variance-stabilizing transformation (VST) and Z-score normalized by row. CK, control; TR, drought treatment. (**B**) A skipped exon (SE) event of *Os03g0700700* detected in DS under drought treatment. The y-axis indicates RNA-seq read coverage, and arcs represent junction reads supporting the splicing event. Asterisks denote genes that are significantly differentially expressed in both DTTR vs DTCK and DSTR vs DSCK

comparisons (adjusted $P < 0.05$ and $|\log_2 FC| \geq 1$).

Discussion

Integrated Evaluation Identifies Drought-Resistant Germplasm at the Rice Seedling Stage

Plant drought resistance involves multiple physiological and morphological strategies, including drought escape, avoidance, tolerance, and post-drought recovery (Gupta et al. 2020). Drought avoidance mainly maintains relatively high water potential through enhanced water uptake by a well-developed root system and reduced water loss via stomatal regulation, whereas drought tolerance emphasizes maintaining metabolic activity under low water potential through osmotic adjustment and antioxidant capacity. Notably, drought-resistant cultivars do not necessarily perform equally well in both avoidance and tolerance, as different genetic backgrounds often favor specific mechanisms. Therefore, a single phenotypic trait is often insufficient to fully capture the complexity of drought. In this study, we evaluated a collection of 283 *indica* rice accessions adapted to the middle and lower reaches of the Yangtze River at the seedling stage under controlled PEG-simulated drought conditions. We measured four key traits (LSRI, LW, DPH, and DRL) and integrated them into CDTM using a fuzzy membership function approach. This multi-trait index allowed us to capture both avoidance- and tolerance-related components of drought response.

LSRI reflects a plant's ability to maintain leaf photosynthetic function and delay senescence under drought stress (Zargar et al. 2022). The LSRI is conceptually similar to the DTD method proposed by Zu et al. (2017), as both quantify green-leaf retention. Higher LSRI suggests less drought-induced leaf damage and stronger stress tolerance. LW is a visible indicator of water deficit and turgor loss, reflecting the capacity of rice leaves to maintain relatively high water status under drought. Leaf rolling can reduce transpirational water loss by decreasing leaf area and radiation

absorption, representing an adaptive response (Wang et al. 2023). Wang et al. (2005) reported that lower LW is associated with higher drought resistance, likely due to more effectively water regulation. Consistent with previous reports, we observed that drought stress significantly increased LW, accompanied by leaf yellowing, rolling, and wilting, particularly in drought-sensitive accessions. Together, these two indices enable a more comprehensive leaf-level assessment of drought tolerance, with LSRI reflecting maintenance of leaf function and LW reflecting maintenance of leaf water status.

PH and RL reflect the plant's adaptive strategies in response to drought stress. Drought stress significantly inhibited PH growth: mean PH decreased from 33.31 cm (CK) to 26.43 cm (TR), with 96.5% of accessions showing reduced PH. In contrast, mean RL increased from 12.19 cm to 13.27 cm under drought , with 69.6% of accessions exhibiting longer roots. This adaptive root growth is consistent with a typical drought-avoidance strategy—enhancing access to deeper water by increasing root length and depth (Uga et al. 2011). Traditional upland rice, grown under rainfed conditions without a hardpan, often develops deeper roots and exhibits stronger drought avoidance. In contrast, lowland rice has historically been cultivated in flooded paddies with restricted root growth due to plow pan, which may impose stronger selection for physiological drought tolerance (Eickhorst and Tippkötter 2009; Kim et al. 2020). These distinct cultivation environments likely shape divergent drought-adaptive mechanisms.

By integrating LSRI, LW, DPH, and DRL into CDTM using a membership function approach, we captured both drought avoidance and tolerance components, providing a more comprehensive and objective evaluation of drought resistance. Based on CDTM, hierarchical clustering and stepwise classification identified 10 extremely drought-tolerant and 15 highly drought-sensitive

accessions. To evaluate the reliability of this classification, we selected *Jiangnongzao 1B* and *TAISEN GLUTINOUS YU 1157* for measurements of antioxidant-related indices. Compared with DS, DT showed higher SOD and POD activities and lower MDA and H_2O_2 levels, suggesting a greater capacity for ROS removal and reduced lipid peroxidation under drought stress, thereby providing physiological support the reliability of the phenotypic classification. The 10 extremely drought-tolerant accessions identified here provide valuable germplasm resources for water-saving and drought-resistant rice breeding targeting the Yangtze River basin, and the associated phenotypic data offer a foundation for subsequent gene discovery.

Multi-omics Integration Prioritizes Candidate Genes for Seedling-Stage Drought Tolerance

Dissecting the genetic basis of drought-related traits is essential for understanding drought adaptation in rice and guiding breeding. In this study, we conducted GWAS using the mrMLM multi-locus framework, which enhance the detecting quantitative trait nucleotides (QTNs) with minor effects. We identified 128 significant SNPs and annotated 133 candidate genes; including 13 previously reported drought-related genes and 22 genes associated with multiple traits. The recovery of known drought-related genes supports the reliability of our association strategy, and pleiotropic loci suggest shared genetic control across different aspects of seedling-stage drought tolerance.

Notably, several identified genes are involved in ABA biosynthesis, spanning, signaling, and hormone crosstalk. *OsAO3*, associated with LSRI, encodes an aldehyde oxidase that catalyzes the final step of ABA biosynthesis. Loss-of-function mutants of *OsAO3* show reduced drought tolerance, whereas overexpression enhances it, indicating that *OsAO3* influences drought tolerance via modulating endogenous ABA levels (Shi et al. 2021). *OsGH3-2 and OsJAZ9,* associated with DRL,

have been reported to affect drought responses through hormone-related regulation of stomatal traits. *OsGH3-2* lowers auxin levels and promotes ABA accumulation, which is linked to stomatal closure, while *OsJAZ9* overexpression increases ABA and JA levels and reduces stomatal density and reduced transpiration (Du et al. 2012; Singh et al. 2021). *OsRNS4*, associated with LW, functions in ABA signaling through interaction with receptor-like kinase *OsASLRK* and phosphorylation (Du et al. 2022). Together, these genes highlight the cental role of ABA in coordinating drought responses at multiple levels.

Several genes identified in this study contribute to leaf morphological and epidermal traits that influence water balance. For instance, *OsHB4* influences leaf rolling and stomatal conductance (Zhang et al. 2018), *OsWR1* promotes wax biosynthesis (Wang et al. 2012), and *LP2* regulates stomatal density (Ahmad et al. 2016). These genes provide a molecular basis for stuctural and physiological traits that contribute to drought resistance.

Integrating GWAS with transcriptomic analysis enhances candidate gene prioritization. Among the 133 GWAS-derived candidates, 69 (51.9%) showed significant differential expression in at least one comparison. Notably, six of these also showed significant expression changes in the independent drought-resistant cultivar *HY73*, reinforcing their potential functional relevance. These genes are involved in phosphate transport (Secco et al. 2010), auxin response (Ma et al. 2023), carotenoid metabolism (Lv et al. 2012), sulfur metabolism (Mou et al. 2015), MAPK signaling, and starch biosynthesis (Akihiro et al. 2005), underscoring the multi-faceted nature of drought responses.

Among the repeatedly detected genes, *Os05g0576800 (OsMPK17)* was associated with LW, LSRI, and CDTM, making it the most frequently identified candidate. *OsMPK17* encodes a MAPK induced under drought stress. Overexpression of *OsMPK17* improves drought tolerance under both

PEG-simulated and soil drought conditions, accompanied by reduced water loss and increased root and shoot length (Li et al. 2020). *OsMPK17* is regulated by ABA and methyl jasmonate, suggesting that MAPK signaling may contribute to integrating hormone cues during drought responses.

At the post-transcriptional level, DAS analysis identified a significant SE event in *Os03g0700700 (OsLOX1)*. *OsLOX1* encodes a *LOX* and has been described as a key enzyme in JA biosynthesis (Xing et al. 2020a), with reported roles in stress responses. JA signaling is activated under drought stress and contributes to stomatal closure, antioxidant defense, ROS scavenging, and osmotic adjustment (Anjum et al. 2011; Fugate et al. 2018). JA and ABA pathways show extensive crosstalk during drought responses, coordinating stomatal behavior and water balance. The drought-associated splicing change in *Os03g0700700* may modulate *LOX* function and thereby influence JA signaling; however, this hypothesis requires experimental validation. Interestingly, *Os03g0700400 (OsLOX4)*, another *LOX* family member, was also among the repeatedly identified genes, further implicating *LOX*-related pathways in seedling drought responses. *LOX* family members have been reported to participate in drought responses in multiple species (Xing et al. 2020b; Weng et al. 2025), supporting the potential role of *Os03g0700700* and *Os03g0700400* in rice

Conclusions

This study established an integrated, multi-trait evaluation framework for seedling-stage drought tolerance in rice and identified 10 extremely drought-tolerant indica accessions. By integrating GWAS and transcriptomic analyses, 12 candidate genes associated with drought tolerance were identified, among which *OsMPK17* and several others were repeatedly detected

across multiple traits, and alternative splicing analysis further revealed a significant skipped exon event in *OsLOX1* under drought stress. Together, these findings provide priority targets and genetic resources for functional validation and marker-assisted breeding aimed at improving drought tolerance in rice.

Abbreviations

DTD Drought tolerance degree

GWAS Genome-wide association studies

ABA Abscisic acid

DRI Drought resistance index

AS Alternative splicing

RNA-seq RNA sequencing

CK Control check

TR Treatment under drought stress

RL Root length

PH Plant height

DRH Drought resistance coefficient of plant height

DRL Drought resistance coefficient of root length

LSRI Leaf senescence resistance index

LW Leaf wilting score

DRC Drought resistance coefficient

CDTM Comprehensive drought tolerance metric

DT *Jiangnongzao 1B*

DS *TAISEN GLUTINOUS YU 1157*

SOD Superoxide dismutase

POD Peroxidase

MDA Malondialdehyde

H_2O_2 Hydrogen peroxide

MAF Minor allele frequency

PCA Principal component analysis

LD Linkage disequilibrium

TPM Transcripts per million

DEGs Differentially expressed genes

GO Gene ontology

KEGG Kyoto encyclopedia of genes and genomes

SE Skipped exon

RI Retained intron

A5SS Alternative 5' splice sites

A3SS Alternative 3' splice sites

MXE Mutually exclusive exons

DAS Differential alternative splicing

FDR False discovery rate

HY73 *Hanyou 73*

JA Jasmonic acid

MAPK Mitogen-activated protein kinase

BP Biological process

MF Molecular function

CC Cellular component

LOX Lipoxygenase

VST Variance-stabilizing transformation

QTN Quantitative trait nucleotide

Supplementary Information

Supplementary Material 1: **Table S1**. Evaluation criteria for leaf wilting degree. **Table S2**. Phenotypic data for five drought-related traits in 283 rice accessions. **Table S3**. Descriptive statistics of traits in 283 rice accessions. **Table S3**. Drought tolerance classification of 283 rice accessions. **Table S5**. Phenotypes of extremely drought-tolerant accessions. **Table S6**. Significant SNPs associated with drought-related traits identified by GWAS. **Table S7**. SNPs significantly associated with multiple drought-related traits. **Table S8**. Candidate genes associated with leaf senescence resistance index. **Table S9**. Candidate Genes associated with leaf wilting score. **Table S10**. Candidate genes associated with DRC of plant height. **Table S11**. Candidate genes associated with DRC of root length. **Table S12**. Candidate genes associated with CDTM. **Table S13**. Candidate genes associated with multiple traits and responsive to drought.

Supplementary Material 2: **Figure S1.** Phenotypic distribution of drought-related traits at the rice seedling stage. **Figure S2.** Hierarchical clustering of 283 indica rice accessions based on seedling-

stage drought tolerance. **Figure S3**. Effect of drought stress on SOD activity and H_2O_2 content in two rice varieties. **Figure S4**. Principal component analysis of 283 rice accessions. **Figure S5**. Quantile-quantile plots for 5 drought-related traits. **Figure S6**. KEGG enrichment analysis of differentially expressed genes in DT and DS. **Figure S7**. Expression heatmap of 12 candidate genes in *Hanyou73.*

Author Contributions

K.X.H. and Y.X.L. and L.Z.L. conceptualized the study. K.X.H. and Y.X.L. and Z.J.L. conducted the formal analyses. H.X.Y., H.Y.Z., D.Z.X. and X.F.Z. acquired and curated the datasets for this study. K.X.H. and Y.X.L. and Z.J.L. prepared the figures and tables. K.X.H. and Y.X.L. drafted the original manuscript. X.F.Z. and L.Z.L. supervised the study and edited the manuscript. All authors have read and approved the final manuscript.

Acknowledgements

We appreciate the editor and anonymous reviewers for their fruitful comments.

Funding

This work was supported by Yuelushan Laboratory Breeding Program (YLS-2025-2Y03018)，Changsha Natural Science Foundation Project (kq2402109) .

Declarations

Competing Interests

The authors declare no competing interests.

Ethical Approval

Not applicable.

Consent To Participate

Not applicable.

Consent for Publication

Not applicable.

Data Availability

The raw sequence data for SNP can be found in the BioProject ID PRJNA321462 (2016-05-13), PRJNA331215 (2016-07-25), and PRJNA734973 (2021-05-22) on NCBI and 3k RGP.The URL is https://www.ncbi.nlm.nih.gov/sra and https://registry.opendata.aws/3kricegenome/. The raw transcriptome sequencing data have been deposited in the Genome Sequence Archive (GSA) of the National Genomics Data Center (NGDC) under accession number CRA039440 (https://ngdc.cncb.ac.cn/gsa/browse/CRA039440).

References

Ahmad I, Devonshire J, Mohamed R, et al (2016) Overexpression of the potassium channel TPK b in small vacuoles confers osmotic and drought tolerance to rice. New Phytol 209:1040–1048. https://doi.org/10.1111/nph.13708

Ahmadikhah A, Marufinia A (2016) Effect of reduced plant height on drought tolerance in rice. 3 Biotech 6:221. https://doi.org/10.1007/s13205-016-0542-3

Akihiro T, Mizuno K, Fujimura T (2005) Gene Expression of ADP-glucose Pyrophosphorylase and Starch Contents in Rice Cultured Cells are Cooperatively Regulated by Sucrose and ABA. Plant Cell Physiol 46:937–946. https://doi.org/10.1093/pcp/pci101

Alexander DH, Novembre J, Lange K (2009) Fast model-based estimation of ancestry in unrelated individuals. Genome Res 19:1655–1664. https://doi.org/10.1101/gr.094052.109

Anjum SA, Wang L, Farooq M, et al (2011) Methyl Jasmonate-Induced Alteration in Lipid Peroxidation, Antioxidative Defence System and Yield in Soybean Under Drought: Methyl Jasmonate and Drought Tolerance in Maize. J Agron Crop Sci 197:296–301. https://doi.org/10.1111/j.1439-037X.2011.00468.x

Bhandari U, Gajurel A, Thapa I, Pokhrel Koshraj (2022) EFFECT OF DROUGHT ON MORPHOPHYSIOLOGICAL TRAITS OF RICE: A REVIEW. Trop Agroecosystems 3:57–62. https://doi.org/10.26480/taec.02.2022.57.62

Bhattacharjee B, Ali A, Rangappa K, et al (2023) A detailed study on genetic diversity, antioxidant machinery, and expression profile of drought-responsive genes in rice genotypes exposed to artificial osmotic stress. Sci Rep 13:18388. https://doi.org/10.1038/s41598-023-45661-8

Chen F, Zhang H, Li H, et al (2023) IPA1 improves drought tolerance by activating SNAC1 in rice. BMC Plant Biol 23:55. https://doi.org/10.1186/s12870-023-04062-9

Dorion S, Ouellet JC, Rivoal J (2021) Glutathione Metabolism in Plants under Stress: Beyond Reactive Oxygen Species Detoxification. Metabolites 11:641. https://doi.org/10.3390/metabo11090641

Du C, Cai W, Lin F, et al (2022) Leucine-rich repeat receptor-like kinase OsASLRK regulates abscisic acid and drought responses via cooperation with S-like RNase OsRNS4 in rice. Environ Exp Bot 201:104949. https://doi.org/10.1016/j.envexpbot.2022.104949

Du H, Wu N, Fu J, et al (2012) A GH3 family member, OsGH3-2, modulates auxin and abscisic acid levels and differentially affects drought and cold tolerance in rice. J Exp Bot 63:6467–6480. https://doi.org/10.1093/jxb/ers300

Eickhorst T, Tippkötter R (2009) Management-induced structural dynamics in paddy soils of south east China simulated in microcosms. Soil Tillage Res 102:168–178. https://doi.org/10.1016/j.still.2008.07.007

Fugate KK, Lafta AM, Eide JD, et al (2018) Methyl jasmonate alleviates drought stress in young sugar beet (*Beta vulgaris* L.) plants. J Agron Crop Sci 204:566–576. https://doi.org/10.1111/jac.12286

Fukai S, Pantuwan G, Jongdee B, Cooper M (1999) Screening for drought resistance in rainfed lowland rice. Field Crops Res 64:61–74. https://doi.org/10.1016/S0378-4290(99)00051-9

Geng A, Lian W, Wang Y, et al (2024) Molecular Mechanisms and Regulatory Pathways Underlying Drought Stress Response in Rice. Int J Mol Sci 25:1185. https://doi.org/10.3390/ijms25021185

Ghazy MI, EL-Naem SA, Hefeina AG, et al (2024) Genome-Wide Association Study of Rice Diversity Panel Reveals New QTLs for Tolerance to Water Deficit Under the Egyptian Conditions. Rice 17:29. https://doi.org/10.1186/s12284-024-00703-1

Guo Z, Yang W, Chang Y, et al (2018) Genome-Wide Association Studies of Image Traits Reveal Genetic Architecture of Drought Resistance in Rice. Mol Plant 11:789–805. https://doi.org/10.1016/j.molp.2018.03.018

Gupta A, Rico-Medina A, Caño-Delgado AI (2020) The physiology of plant responses to drought. Science 368:266–269. https://doi.org/10.1126/science.aaz7614

Hou Q, Ufer G, Bartels D (2016) Lipid signalling in plant responses to abiotic stress. Plant Cell Environ 39:1029–1048. https://doi.org/10.1111/pce.12666

Huang S, Liu M, Chen G, et al (2022) Favorable QTLs from Oryza longistaminata improve rice drought resistance. BMC Plant Biol 22:136. https://doi.org/10.1186/s12870-022-03516-w

Huang X, Wei X, Sang T, et al (2010) Genome-wide association studies of 14 agronomic traits in rice landraces. Nat Genet 42:961–967. https://doi.org/10.1038/ng.695

Jarin AS, Islam MdM, Rahat A, et al (2024) Drought Stress Tolerance in Rice: Physiological and Biochemical Insights. Int J Plant Biol 15:692–718. https://doi.org/10.3390/ijpb15030051

Kim D, Langmead B, Salzberg SL (2015) HISAT: a fast spliced aligner with low memory requirements. Nat Methods 12:357–360. https://doi.org/10.1038/nmeth.3317

Kim Y, Chung YS, Lee E, et al (2020) Root Response to Drought Stress in Rice (Oryza sativa L.). Int J Mol Sci 21:1513. https://doi.org/10.3390/ijms21041513

Li H, Durbin R (2009) Fast and accurate short read alignment with Burrows-Wheeler transform. Bioinforma Oxf Engl 25:1754–1760. https://doi.org/10.1093/bioinformatics/btp324

Li L-Y, Lan J-P, Yang M, et al (2020) Overexpression of OsMPK17 protein enhances drought tolerance of rice. Acta Agron Sin 46:20–30. https://doi.org/10.3724/SP.J.1006.2020.92007

Li R, Zeng Y, Xu J, et al (2015) Genetic variation for maize root architecture in response to drought stress at the seedling stage. Breed Sci 65:298–307. https://doi.org/10.1270/jsbbs.65.298

Li X, Guo Z, Lv Y, et al (2017) Genetic control of the root system in rice under normal and drought stress conditions by genome-wide association study. PLOS Genet 13:e1006889. https://doi.org/10.1371/journal.pgen.1006889

Liu T, Li S, Du H, et al (2024) The Identification of Drought Tolerance Candidate Genes in Oryza sativa L. ssp. Japonica Seedlings through Genome-Wide Association Study and Linkage Mapping. Agriculture 14:603. https://doi.org/10.3390/agriculture14040603

Love MI, Huber W, Anders S (2014) Moderated estimation of fold change and dispersion for RNA-seq data with DESeq2. Genome Biol 15:550. https://doi.org/10.1186/s13059-014-0550-8

Lu GH, Dai JR, Zhang SK, et al (2005) Comparative drought tolerance of Chinese backbone maize inbred lines under different drought stress conditions. Acta Agron Sin 31:1284–1288

Lv M-Z, Chao D-Y, Shan J-X, et al (2012) Rice Carotenoid β-Ring Hydroxylase CYP97A4 is Involved in Lutein Biosynthesis. Plant Cell Physiol 53:987–1002. https://doi.org/10.1093/pcp/pcs041

Ma F, Zhang F, Zhu Y, et al (2023) Auxin signaling module OsSK41-OsIAA10-OsARF regulates grain yield traits in rice. J Integr Plant Biol 65:1753–1766. https://doi.org/10.1111/jipb.13484

McKenna A, Hanna M, Banks E, et al (2010) The Genome Analysis Toolkit: A MapReduce framework for analyzing next-generation DNA sequencing data. Genome Res 20:1297–1303. https://doi.org/10.1101/gr.107524.110

Mou S, Shi L, Lin W, et al (2015) Over-Expression of Rice CBS Domain Containing Protein, OsCBSX3, Confers Rice Resistance to Magnaporthe oryzae Inoculation. Int J Mol Sci 16:15903–15917. https://doi.org/10.3390/ijms160715903

Panda D, Mishra SS, Behera PK (2021) Drought Tolerance in Rice: Focus on Recent Mechanisms and Approaches. Rice Sci 28:119–132. https://doi.org/10.1016/j.rsci.2021.01.002

Purcell S, Neale B, Todd-Brown K, et al (2007) PLINK: a tool set for whole-genome association and population-based linkage analyses. Am J Hum Genet 81:559–575. https://doi.org/10.1086/519795

Roberts A, McMillan L, Wang W, et al (2007) Inferring missing genotypes in large SNP panels using fast nearest-neighbor searches over sliding windows. Bioinforma Oxf Engl 23:i401-407. https://doi.org/10.1093/bioinformatics/btm220

Secco D, Baumann A, Poirier Y (2010) Characterization of the Rice *PHO1* Gene Family Reveals a Key Role for *OsPHO1;2* in Phosphate Homeostasis and the Evolution of a Distinct Clade in Dicotyledons. Plant Physiol 152:1693–1704. https://doi.org/10.1104/pp.109.149872

Shen S, Park JW, Lu Z, et al (2014) rMATS: robust and flexible detection of differential alternative splicing from replicate RNA-Seq data. Proc Natl Acad Sci U S A 111:E5593-5601. https://doi.org/10.1073/pnas.1419161111

Shi F, Dong Y, Wang M, Qiu D (2020) Transcriptomics analyses reveal that OsMIOX improves rice drought tolerance by regulating the expression of plant hormone and sugar related genes. Plant Biotechnol Rep 14:339–349. https://doi.org/10.1007/s11816-020-00608-7

Shi X, Tian Q, Deng P, et al (2021) The rice aldehyde oxidase OsAO3 gene regulates plant growth, grain yield, and drought tolerance by participating in ABA biosynthesis. Biochem Biophys Res Commun 548:189–195. https://doi.org/10.1016/j.bbrc.2021.02.047

Singh AP, Mani B, Giri J (2021) OsJAZ9 is involved in water-deficit stress tolerance by regulating leaf width and stomatal density in rice. Plant Physiol Biochem 162:161–170. https://doi.org/10.1016/j.plaphy.2021.02.042

Sun X, Xiong H, Jiang C, et al (2022) Natural variation of DROT1 confers drought adaptation in upland rice. Nat Commun 13:4265. https://doi.org/10.1038/s41467-022-31844-w

Tamura K, Stecher G, Kumar S (2021) MEGA11: Molecular Evolutionary Genetics Analysis Version 11. Mol Biol Evol 38:3022–3027. https://doi.org/10.1093/molbev/msab120

Uga Y, Okuno K, Yano M (2011) Dro1, a major QTL involved in deep rooting of rice under upland field conditions. J Exp Bot 62:2485–2494. https://doi.org/10.1093/jxb/erq429

Wang W, Mauleon R, Hu Z, et al (2018) Genomic variation in 3,010 diverse accessions of Asian cultivated rice. Nature 557:43–49. https://doi.org/10.1038/s41586-018-0063-9

Wang X, Huang J, Peng S, Xiong D (2023) Leaf rolling precedes stomatal closure in rice (Oryza sativa) under drought conditions. J Exp Bot 74:6650–6661. https://doi.org/10.1093/jxb/erad316

Wang Y, Wan L, Zhang L, et al (2012) An ethylene response factor OsWR1 responsive to drought stress transcriptionally activates wax synthesis related genes and increases wax production in rice. Plant Mol Biol 78:275–288. https://doi.org/10.1007/s11103-011-9861-2

Wang YH, Yao YQ, Zhang CJ, et al (2005) Study on drought-resistance identification methods and evaluation index of dry-land rice—Evaluation of drought-resistance of dry-land rice in seeding stage. Agric Res Arid Areas 23:134–137, 164

Wasternack C, Song S (2016) Jasmonates: biosynthesis, metabolism, and signaling by proteins

activating and repressing transciption. J Exp Bot erw443. https://doi.org/10.1093/jxb/erw443
Wei H, Lou Q, Xu K, et al (2017) Alternative splicing complexity contributes to genetic improvement of drought resistance in the rice maintainer HuHan2B. Sci Rep 7:11686. https://doi.org/10.1038/s41598-017-12020-3
Wei X, Cang B, Yu K, et al (2022) Physiological Characterization of Drought Responses and Screening of Rice Varieties under Dry Cultivation. Agronomy 12:2849. https://doi.org/10.3390/agronomy12112849
Weng Y, Wang Y, Wang K, et al (2025) OsLOX1 positively regulates seed vigor and drought tolerance in rice. Plant Mol Biol 115:16. https://doi.org/10.1007/s11103-024-01543-9
Xing Q, Liao J, Cao S, et al (2020a) CmLOX10 positively regulates drought tolerance through jasmonic acid -mediated stomatal closure in oriental melon (Cucumis melo var. makuwa Makino). Sci Rep 10:17452. https://doi.org/10.1038/s41598-020-74550-7
Xing Q, Liao J, Cao S, et al (2020b) CmLOX10 positively regulates drought tolerance through jasmonic acid -mediated stomatal closure in oriental melon (Cucumis melo var. makuwa Makino). Sci Rep 10:17452. https://doi.org/10.1038/s41598-020-74550-7
Yang H, Li P, Jin G, et al (2022a) Temporal regulation of alternative splicing events in rice memory under drought stress. Plant Divers 44:116–125. https://doi.org/10.1016/j.pld.2020.11.004
Yang Y, Zhang C, Zhu D, et al (2022b) Identifying candidate genes and patterns of heat-stress response in rice using a genome-wide association study and transcriptome analyses. Crop J 10:1633–1643. https://doi.org/10.1016/j.cj.2022.02.011
Yoshida S, Forno D, Cock J (1971) Laboratory manual for physiological studies of rice
Zargar SM, Mir RA, Ebinezer LB, et al (2022) Physiological and Multi-Omics Approaches for Explaining Drought Stress Tolerance and Supporting Sustainable Production of Rice. Front Plant Sci 12:803603. https://doi.org/10.3389/fpls.2021.803603
Zhang C, Dong S-S, Xu J-Y, et al (2019a) PopLDdecay: a fast and effective tool for linkage disequilibrium decay analysis based on variant call format files. Bioinforma Oxf Engl 35:1786–1788. https://doi.org/10.1093/bioinformatics/bty875
Zhang J, Zhang H, Srivastava AK, et al (2018) Knockdown of Rice MicroRNA166 Confers Drought Resistance by Causing Leaf Rolling and Altering Stem Xylem Development. Plant Physiol 176:2082–2094. https://doi.org/10.1104/pp.17.01432
Zhang Y-M, Jia Z, Dunwell JM (2019b) Editorial: The Applications of New Multi-Locus GWAS Methodologies in the Genetic Dissection of Complex Traits. Front Plant Sci 10:100. https://doi.org/10.3389/fpls.2019.00100
Zhang Y-W, Tamba CL, Wen Y-J, et al (2020) mrMLM v4.0.2: An R Platform for Multi-locus Genome-wide Association Studies. Genomics Proteomics Bioinformatics 18:481–487. https://doi.org/10.1016/j.gpb.2020.06.006
Zhao S, Ye Z, Stanton R (2020) Misuse of RPKM or TPM normalization when comparing across samples and sequencing protocols. RNA N Y N 26:903–909. https://doi.org/10.1261/rna.074922.120
Zong W, Tang N, Yang J, et al (2016) Feedback Regulation of ABA Signaling and Biosynthesis by a bZIP Transcription Factor Targets Drought-Resistance-Related Genes. Plant Physiol 171:2810–2825. https://doi.org/10.1104/pp.16.00469
Zu X, Lu Y, Wang Q, et al (2017) A new method for evaluating the drought tolerance of upland rice cultivars. Crop J 5:488–498. https://doi.org/10.1016/j.cj.2017.05.002

Supplementary Files

This is a list of supplementary files associated with this preprint. Click to download.

- SupplementaryMaterial1.xlsx
- SupplementaryMaterial2.docx
- FigS1.tif
- FigS2.png
- FigS3.png
- FigS4.png
- FigS5.png
- FigS6.png
- FigS7.png